Excitation of Autoionization States in O2 by Using High-Order Harmonics

Article *in* Journal- Korean Physical Society · July 2006

CITATIONS
2

READS
173

8 authors, including:

Kyung Taec Kim
Gwangju Institute of Science and Technology
75 PUBLICATIONS **1,023** CITATIONS
SEE PROFILE

E. Krishnakumar
Raman Research Institute
143 PUBLICATIONS **2,122** CITATIONS
SEE PROFILE

Mi Na Park
41 PUBLICATIONS **238** CITATIONS
SEE PROFILE

Tayyab Imran
COMSATS University Islamabad
46 PUBLICATIONS **187** CITATIONS
SEE PROFILE

Journal of the Korean Physical Society, Vol. 49, No. 1, July 2006, pp. 309∼313

Excitation of Autoionization States in O_2 by Using High-Order Harmonics

Kyung Taec Kim,* Kyung Sik Kang, Mi Na Park, Tayyab Imran, Changjun Zhu and Chang Hee Nam
Department of Physics and Coherent X-ray Research Center, Korea Advanced Institute of Science and Technology, Daejeon 305-701

E. Krishnakumar
Tata Institute of Fundamental Research, Homi Bjabha Road, Mumbai-400005, India

G. Umesh
Physics Department, National Institute of Technology Karnataka, Surathkal, Mangalore 575025, India.

(Received 25 January 2006)

Photoionization of oxygen molecules by high-order harmonics was investigated. High-order harmonics of a Ti:sapphire laser produced in a Kr gas cell were used to excite autoionization states of O_2. Since the high-order harmonic source used contains several harmonic orders, the resulting photoelectron spectrum also showed multiple peaks coming from different orders of harmonics. A subtraction method using known photoionization cross-sections was employed to separate out individual contributions from the harmonics. The photoelectron spectrum from the 11th harmonic shows a clean contribution from an autoionizing state.

PACS numbers: 42.65.K, 33.60.Cv
Keywords: Oxygen molecule, Autoionization, High-order harmonics, Photoelectron spectroscopy

I. INTRODUCTION

Photoionization of O_2 has been extensively investigated for the last few decades by using synchrotron radiation and other more conventional light sources like discharge tubes [1–7]. These experiments have involved total ionization cross-sections using ion mass spectrometry and partial ionization cross-sections using photoelectron spectroscopy. The ionization of O_2 yields several electronic states of the O_2^+ ion, depending on the photon energy [8]. The ionization continuum of O_2, like any other molecule, shows a large number of discrete states [9]. These states, also called autoionizing states, are neutral excited states lying above the first ionization limit and have finite lifetimes before they decay through electron ejection. Thus, a final positive ionic state may be accessed through direct ionization or indirect ionization through a two-step process. In this two-step process, the first step involves excitation of the autoionizing state, and in the second step, this state decays producing an electron and a final positive ionic state. Some of these autoionizing states have been studied using photoelectron spectroscopy. The most notable one of them has been the autoionizing state located at about 73.5 nm, which could be accessed by one of the Ne I emission lines and which shows rather spectacular changes in the vibrational intensity pattern in the formation of the O_2^+ $X^2\Pi_g$ ground state, as compared to direct ionization [10].

The availability of ultrafast and coherent extreme ultra violet (XUV) radiation produced by high-order harmonic generation (HHG) has given a new impetus to the study of the photoionization of atoms and molecules. One of the great advantages of XUV radiation obtained from HHG is that its pulse width can reach a few hundred attoseconds. Therefore, it is an ideal tool to study the ultra fast electron dynamics in atoms and molecules. Furthermore, the photon energy of the harmonics can be adjusted within a certain range. Use of coherent XUV radiation for probing electron dynamics in atoms has been demonstrated in recent times [11,12]. However, similar experiments on molecules are yet to be done. In this context, we have initiated the use of short, pulsed, coherent XUV to investigate the ionization of molecules. In this paper, we present the results of our work in obtaining the photoelectron spectra of O_2 by using several harmonics and the identification of the autoionizing contribution at a particular harmonic.

II. EXPERIMENTS AND DISCUSSION

HHG is generally carried out by focusing a short-pulsed laser beam into a rare gas cell. The HHG may be well explained by using a semi-classical model. An

*E-mail: kyungtaec@kaist.ac.kr; Fax: +82-42-869-2510

electron tunnels out through the atomic potential well, which is modulated severely by the strong laser field. The ionized electron is then accelerated by the intense laser field, and it returns to the atomic core as the laser field is reversed in the next half cycle. A photon of energy equal to the sum of the kinetic energy of the electron and the ionization potential of the atom is emitted as the electron is recombined with the atomic core. Since this procedure is repeated, but in the other direction, at every half cycle of the laser pulse, constructive interference occurs only for odd harmonics of the fundamental laser pulse. The resulting harmonics consist of odd harmonics of the fundamental laser. Very high-order harmonics have been produced by this technique, reaching all the way up to the soft X-ray region [13]. These are suitable to ionize atoms and molecules. For example, the 9th harmonic of the Ti:sapphire laser has an energy of 13.5 eV and is enough to ionize O_2 molecules. Since the electron path is determined by the electric field of the fundamental laser, the recombined electron energy can change if the laser wavelength changes. Since we use a Ti:sapphire laser system using a chirped pulse amplification technique, there are a pair of gratings after the amplifier. The chirp of the laser can be controlled by adjusting the distance between the two gratings. For example, the laser pulses are positively chirped if we decrease the grating distance. In this case, the frequency of the beginning part of the laser pulse is lower than that of the tail. Since high-order harmonics are generated at the beginning of the laser pulse because of the ionization, the energy of each harmonic can be changed within a certain range by changing the chirp of the laser. This fine tunability using the chirp of the fundamental frequency is used to optimize the transition to an autoionizing state in our experiment. Like in the case of electronic excitation, ionization is also governed in molecules by the Born-Oppenheimer approximation leading to Franck-Condon rule for transitions. Thus, all the vibrational levels of the positive molecular ionic states that have nonzero overlap with the initial vibrational level of the neutral molecule are populated during photoionization, with the intensity distribution depending on the magnitude of the overlap. Thus, the photoelectron spectra resulting from direct ionization give vibrational populations in each of the electronic states, which are within the available energy, according to the Frank-Condon rule. During the early days of photoelectron spectroscopy, a deviation from this was observed at certain photon wavelengths for a given molecule. Soon this was realized as being due to excitation of autoionizing states lying in the continuum. If the autoionizing state has a lifetime that is larger than vibrational motion, the excited molecule will have changed its internuclear separation before the electron is ejected. The resulting vibrational level intensities seen in the photoelectron spectra will then correspond to the Franck-Condon overlap of the autoionizing state with those of the positive ion states of the molecule at the time of electron ejection. This will lead to a different intensity distribution in the photoelectron spectra than that obtained by direct ionization [10].

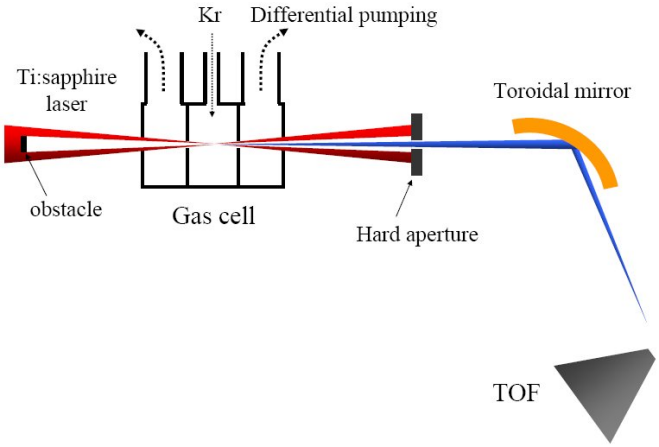

Fig. 1. Schematic of the experimental setup.

The schematic of our experimental setup is shown in Fig.1. A 1-kHz 6-mJ 25-fs 800-nm Ti:sapphire laser beam is used to generate XUV radiation. The laser beam size is adjusted with an 8-mm hard aperture, and the central part of the beam is blocked with an optical obstacle. Therefore, the spatial beam pattern is annular so that we can spatially filter out the laser beam with a hard aperture after the harmonic generation. The annular beam is focused into a Kr-filled gas cell for the harmonic generation. The laser pulse energy used for harmonic generation is 0.8 mJ. The gas cell is specially designed as shown in Fig. 1 to reduce the gas leakage into the main vacuum chamber. The gas target consists of 3 cells. The first and the third cells are 8-mm-thick, and they are directly connected to a scroll pump for the differential pumping between the second gas cell and the main vacuum chamber. The target gas, krypton, is put into the central gas cell so that we can increase the gas pressure of the cell without much load on the turbo pump connected to the main vacuum chamber. The pressure of the target gas is controlled by using a flow controller which has a feedback loop. After that, it is controlled by using a needle valve again. Therefore, the pressure of the harmonic target can be maintained constant for several hours. The XUV radiation generated in the second gas cell is re-focused by using a gold-coated toroidal focusing mirror into an ultra-high-vacuum chamber, such that it intersects an effusive molecular beam of O_2 at the focal spot. The effusive beam is produced by using a capillary and is skimmed and differentially pumped to obtain a well-defined molecular beam. A 1-m-long magnetic bottle time-of-flight spectrometer is used to analyze the photoelectron energy. The electrons are detected by using a pair of microchannel plates of 40 mm in diameter in a chevron configuration. After suitable amplification, the data is collected in a storage digital oscilloscope with a timing bin resolution of 0.5 ns.

The photoelectron spectrometer is energy calibrated

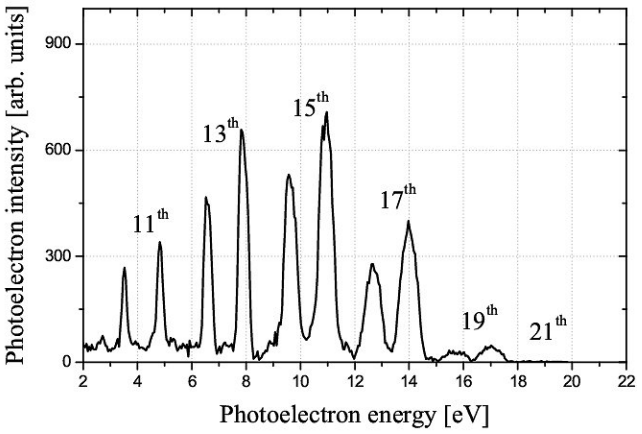

Fig. 2. Photoelectron spectrum of Xe obtained using harmonics ranging from 11th to 21th. Each of the harmonics gives rise to two peaks corresponding to the $^2P_{3/2}$ and the $^2P_{1/2}$ states of Xe^+.

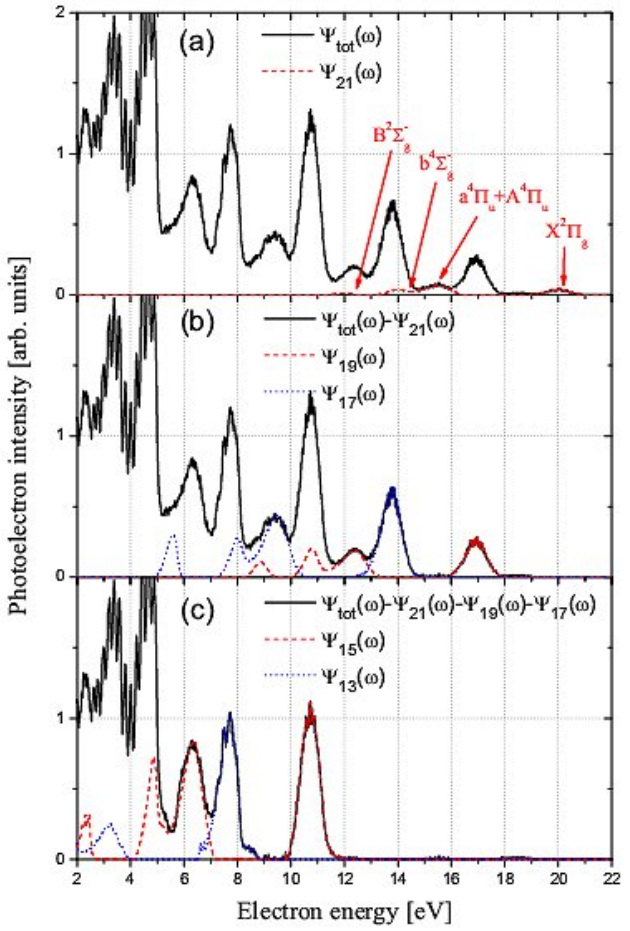

Fig. 3. Photoelectron spectrum of O_2 using harmonic ranging from 9th to 21st. In (a) $\Psi_{tot}(\omega)$ is shown as a solid line, and $\Psi_{21}(\omega)$ is shown as a dotted line. The photoelectron spectra $\Psi_n(\omega)$ subtracted from $\Psi_{tot}(\omega)$ are shown (b) and (c), as described in text.

using photoelectron spectra from Xe obtained using the

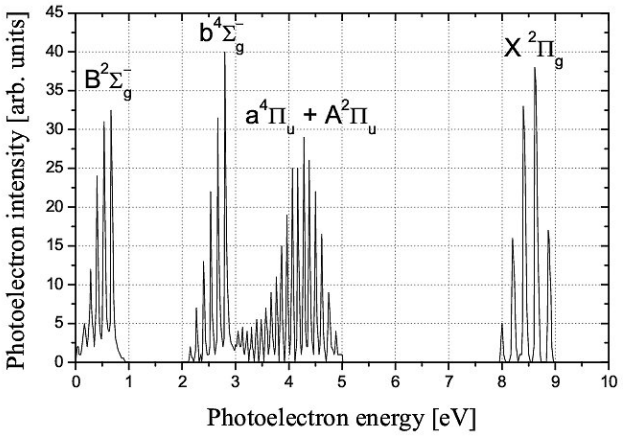

Fig. 4. Synthesized photoelectron spectrum of O_2 obtained with 58.4 nm radiation. The four bunches of vibrational levels correspond to five different electronic states, a shown in the figure, of O_2^+ formed by the photoionization process [2].

high-order harmonics from the 11th to the 21st as shown in Fig. 2. The constant separation between the $^2P_{3/2}$ and the $^2P_{1/2}$ peaks from Xe is used for this purpose as the calibrating scale. The energy resolution, E, of the electron spectrometer as a function of the electron energy can also be obtained by measuring the full width at half maximum of the peaks in the spectra. The photoelectron spectrum of O_2 obtained with the harmonics in the XUV region is shown in Fig. 3 as a function of the electron energy under similar conditions, but for a change in the target gas from Xe to O_2. The spectrum is seen to be a mixture of a large number of photoelectron bands from the several harmonics present in the XUV beam. From the ionization potential of O_2 and the largest photoelectron peak of reasonable intensity seen in the data, harmonics as high as the 21st contribute to the spectrum. We also note that the lowest harmonic energetic enough to ionize O_2 is the 9th.

It appears to be a very complex task to analyze the above spectrum and to separate out the contribution due to each harmonic, considering that each of the harmonics can give rise to at least four dominant vibrational sequences corresponding to the five electronic states of O_2^+ that will be formed in the ionization process over most of the photon energy range under consideration. For the purpose of clarity, we present in Fig. 4 a synthesized photoelectron spectra corresponding to the photon energy of 58.4 nm, which is available in the literature. At higher energies, for example at 30 nm, four more states can enter the picture. However, their contributions are relatively weak in the photon energy range we are interested in, as can be seen from the cross-section summed over all vibrational levels for the formation of each of the electronic states (known as the partial photoionization cross-section) as a function of the photon energy given in Fig. 5. However, the seemingly difficult task has been accomplished by using a systematic

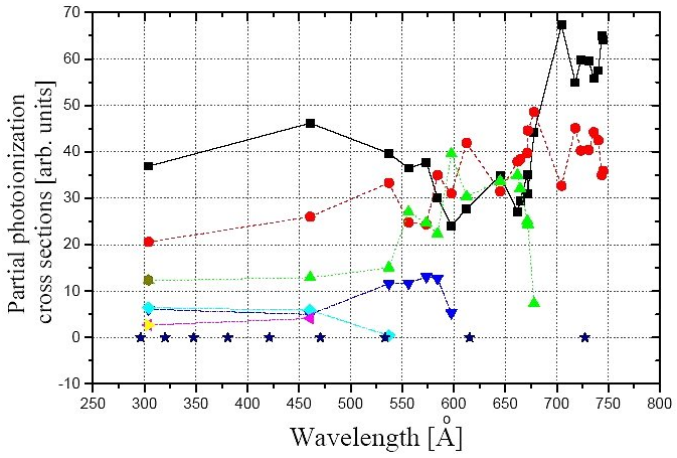

Fig. 5. Partial photoionization cross-sections for O_2 as a function of wavelength (from [1]). They are shown as squares ($X^2\Pi_g$), circles ($a^4\Pi_u + A^2\Pi_u$), triangles ($b^4\Sigma_g^-$), inverted triangles ($B^4\Sigma_g^-$), diamonds ($^2\Pi_u$), triangle directed to the left ($c^4\Sigma_u^-$), triangles directed to the right ($^2\Sigma_u^-$), and pentagons ($^{2,4}\Sigma_g^-$). The harmonic wavelengths from the 11th (extreme right) to the 27th are shown as stars.

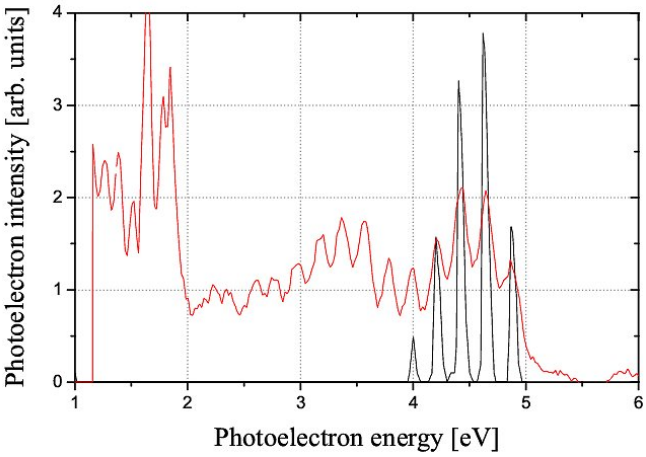

Fig. 6. Comparison of the autoionization and the direct ionization spectra of O_2. The region between 2 eV to 5 eV covers the vibrational bands due to the ground state of O_2^+ ($X^2\Pi_g$) produced by the 11th harmonic. The electron spectrum resulting from direct ionization, taken from literature, is also given for comparison. The contribution due to the autoionization can clearly be seen in the energy range between 2 eV and 4 eV.

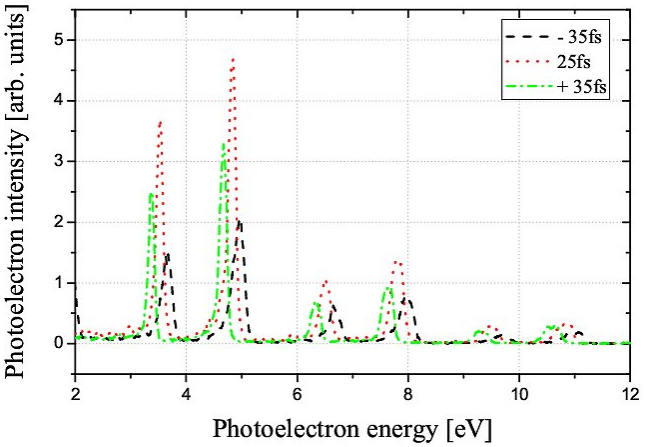

Fig. 7. Chirp dependence of the Xe photoelectron spectrum. The photoelectron spectra are shown as dashed, solid, and dotted lines for –35 fs, 25 fs, and +35 fs, respectively. The sign in front of the pulsewidth is the sign of the chirp.

subtraction of the individual harmonics, starting from the highest, from the total spectrum. The measured total photoelectron spectrum, $\Psi_{tot}(\omega)$, is the sum of the photoelectron spectra, $\Psi_n(\omega)$. Here, $\Psi_n(\omega)$ is the photoelectron spectrum ionized by the nth harmonic. In order to calculate $\Psi_n(\omega)$, we make use of the spectrometer energy resolution obtained from Fig. 2, the photoelectron spectrum given in Fig. 4, and the partial ionization cross-sections given in Fig. 5. To start with, we consider the 21st harmonic. The highest energy peak of $\Psi_{21}(\omega)$ would be that due to the $X^2\Pi_g$ state of O_2^+. Thus, the highest energy peak in $\Psi_{tot}(\omega)$ would be entirely due to this state. These data are then used to generate the contribution due to the four higher-lying states of O_2^+ by using the partial ionization cross-section data given in Fig. 5 and the photoelectron band intensity distribution given in Fig. 3(a) after it is convoluted with the energy resolution function of the spectrometer. This resolution function is taken to be Gaussian with the half width determined from the Xe data given in Fig. 2. The total photoelectron spectrum $\Psi_n(\omega)$ and the calculated photoelectron spectrum $\Psi_{21}(\omega)$ are shown in Fig. 3(a). The $\Psi_{21}(\omega)$ is then subtracted from $\Psi_{tot}(\omega)$. The remaining spectrum corresponds to contributions up to the 19th harmonic. This process is then repeated till we are left with contributions from the 9th and the 11th harmonics only, as shown in Figs. 3(b) and (c). These data are given in Fig. 6, which clearly show the contribution from the autoionizing state excited by the 11th harmonic.

Direct ionization is known to yield the five vibrational levels between 4 and 5 eV, as shown in the spectrum taken from the literature. All the vibrational levels seen between 2 and 4 eV are populated through autoionization, as have been observed before [10].

We also investigated the effect of chirp on the photoelectron spectra. To begin with, the photoelectron spectra of Xe are taken under different conditions of chirp. These are shown in Fig. 7. The energy shift in the photoelectron spectrum as a function of chirp can be clearly seen in the figure. It is also noticed that the spectral energy width is larger in the case of positive chirp as compared to the other two, as manifested in the width of the peaks. Similar data obtained for O_2 are shown in Fig. 8. The noticeable feature in the figure is the smoothening of the vibrational intensity distribution (dotted line) in the autoionized part of the spectrum when the chirp is

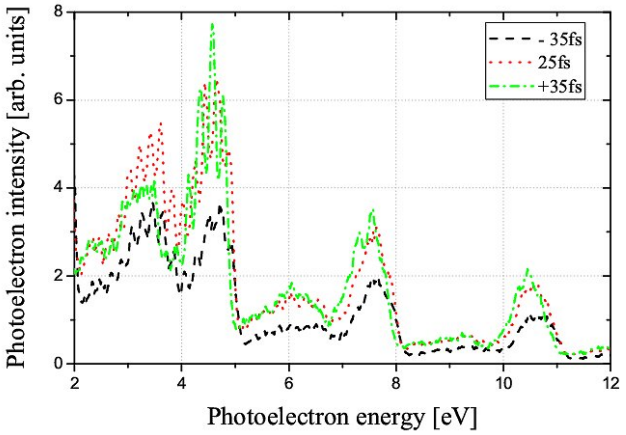

Fig. 8. Chirp dependence of the O_2 photoelectron spectrum. The autoionization peaks from 2 eV to 4 eV are clearly resolved for the –35-fs and the 25-fs cases.

negative. It is as yet unclear how the chirp conditions affects the autoionizing state.

III. CONCLUSIONS

In conclusion, we have studied the photoionization of O_2 by using high-order harmonics of a Ti:sapphire laser produced in a Kr gas cell. The photoelectrons generated in the process were analyzed using a magnetic bottle time-of-flight spectrometer. The contributions from different harmonics were separated out by using a subtraction procedure that employed the instrumental energy resolution function and the existing photoionization data. A clear sign of an autoionizing state was observed in the ionization by the 11th harmonic. The effect of the chirp of the fundamental frequency on the ionization process was also investigated in an effort to fine tune the XUV energy to match the autoionizing state.

ACKNOWLEDGMENTS

This research was supported by the Ministry of Science and Technology of Korea through the Creative Research Initiative Program.

REFERENCES

[1] J. Berkowitz, *Photoabsorption, Photoionization and Photoelectron Spectroscopy* (Academic Press, New York, 1979), p. 101.
[2] D. W. Turner, C. Baker, A. D. Baker and C. R. Brundle, *Molecular Photoelectron Spectroscopy* (Wiley - Interscience, London, 1970), p. 36.
[3] Y. Hikosaka, P. Lablanquie, M. Ahmad, R. I. Hall, J. G. Lambourne, F Penent and J. H. D. Eland, Phys. B: At. Mol. Opt. Phys. **36**, 4311 (2003).
[4] A. V. Golovin, F. Heiser, C. J. K. Quayle, P. Morin, M. Simon, O. Gessner, P.-M. Guyon and U. Becker, Phys. Rev. Lett. **79**, 4554 (1997).
[5] L. Beeching, A. De Fanis, J. M. Dyke, S. D. Gamblin, N. Hooper and A. Morris, J. Chem. Phys. **112**, 1707 (2000).
[6] S. J. Kang, Y. Yi, C. Y. Kim and C. N. Whang, J. Korean Phys. Soc. **46**, 1148 (2005).
[7] Dae-Soung Kim, J. Korean Phys. Soc. **44**, 260 (2004).
[8] O. Edqvist, E. Lindholm, L. E. Selin and L. Åsbrink, Phys. Scripta **1**, 25 (1970).
[9] P. M. Dehmer and W. A. Chupka, J. Chem. Phys. **62**, 4525 (1975).
[10] Vijay Kumar and E. Krishnakumar, J. Electron Spectrosc. Relat. Phenom. **22**, 109 (1981).
[11] M. Drescher, M. Hentschel, R. Kienberger, M. Uiberacker, V. Yakovlev, A. Scrinzi, Th. Westerwalbesloh, U. Kleineberg, U. Heinzmann and F. Krausz, Nature **419**, 803 (2002).
[12] R. Kienberger, M. Hentschel, M. Uiberacker, Ch. Spielmann, M. Kitzler, A. Scrinzi, M. Wieland, Th. Westerwalbesloh, U. Kleineberg, U. Heinzmann, M. Drescher and F. Krausz, Science **297**, 1144 (2002).
[13] Chang Hee Nam, Dong Gun Lee, Jung-Hoon Kim, Yong Ho Cha and Il Woo Choi, J. Korean Phys. Soc. **39**, 873 (2001).